Nonblinking Emitters with Nearly Lifetime-Limited Linewidths in CVD Nanodiamonds

Ke Li,[1] Yu Zhou,[1] A. Rasmita,[1] I. Aharonovich,[2,*] and W. B. Gao[1,†]

[1]*Division of Physics and Applied Physics, School of Physical and Mathematical Sciences, Nanyang Technological University, Singapore 637371, Singapore*

[2]*School of Mathematical and Physical Sciences, University of Technology Sydney, Ultimo, New South Wales 2007, Australia*

(Received 25 March 2016; published 11 August 2016)

Near transform-limited single-photon sources are required for perfect photon indistinguishability in quantum networks. Having such sources in nanodiamonds is particularly important since it can enable engineering hybrid quantum-photonic systems. In this paper, we report the generation of optically stable, nearly transform-limited single silicon-vacancy emitters in nanodiamonds. Lines as narrow as 325 MHz are reported, which is close to the lifetime-limited linewidth (141 MHz). Moreover, the emitters exhibit minimal spectrum diffusion and high photostability, even if pumped well above saturation. Our results suggest that nanodiamonds can host color centers with superior properties suitable for hybrid photonic devices and quantum information.

DOI: 10.1103/PhysRevApplied.6.024010

I. INTRODUCTION

Fluorescent nanodiamonds that host bright and narrow-band optical defects are attractive for numerous applications spanning quantum photonics [1–3], sensing [4–7], and bioimaging [8–10]. One of these defects is the negatively charged silicon vacancy (SiV^-) that has been subject to intense research efforts due to its promising optical properties [11–19]. The defect consists of an interstitial silicon atom splitting two vacancies with a strong zero-phonon line (ZPL) at 738 nm [20]. The structure of the defect is shown schematically in Fig. 1(a). It has a high Debye-Waller factor that results in ∼70% of the emitted photons being into the ZPL, and therefore is suitable for a variety of photonic applications. Because of its inversion symmetry, the defect is not susceptible to electric field fluctuations, and therefore exhibits promising spectral characteristics [15].

For many applications, including quantum bioimaging, sensing, and hybrid quantum photonics, the use of nanodiamonds is preferred [21,22]. This is because nanodiamonds can be easily put to a position of choice, for instance, onto a photonic resonator, to achieve Purcell enhancement [23]. Nanodiamonds can also be positioned onto 1D waveguides such as tapered optical nanofibers [24]. So far, only the nitrogen-vacancy centers and the chromium centers in nanodiamonds have been studied using fluorescence resonant excitation (PLE) [25–27], but the emitters' linewidths were always broadened by strain or significant spectral diffusion that resulted in the majority of lines being broader than 1 GHz.

In this work, we report on nearly lifetime-limited characteristics of the SiV defects in nanodiamonds grown using the chemical vapor deposition (CVD) method. The studied SiV emitters exhibit linewidths as narrow as 325 MHz and high photostability even when excited above saturation. The grown nanodiamonds with such ideal properties will be promising sources for a variety of applications spanning quantum photonics, communications, and quantum sensing.

II. EXPERIMENT

The SiV^- defects are incorporated into the diamond nanocrystals during microwave-plasma CVD growth from 4- to 6-nm nanodiamond seeds (Nanoamor) dispersed in methanol. A clean silicon wafer with a native oxide layer is used as a growth substrate. The nanodiamond seeds are dispersed on the substrate using the spin-coating method and dried under nitrogen flow. The growth conditions are a hydrogen-to-methane ratio of 100∶1 at 60 Torr, with a microwave power of 900 W. Under these conditions, well-faceted nanodiamonds with sizes between 100 and 300 nm can be grown, as shown in Fig. 1(b). The incorporation of silicon into the nanodiamonds occurs during the growth. The origin of the silicon is the substrate, that under these growth conditions is slightly etched [28].

The experimental setup used to characterize the nanodiamonds is shown in Fig. 1(c). The sample is mounted on a stage which is fixed on top of stacked XYZ steppers (Attocube) with nanometer precision. Both the sample

*Igor.Aharonovich@uts.edu.au
†wbgao@ntu.edu.sg

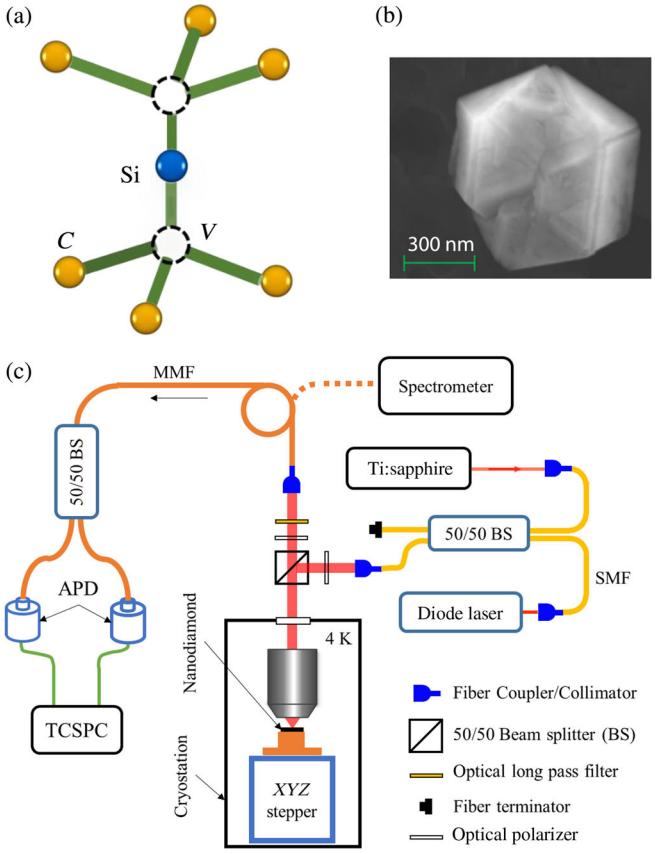

FIG. 1 (a) Schematic illustration of the silicon-vacancy defect. An interstitial silicon atom splits two vacancies in a diamond lattice. (b) Scanning electron microscopy image of a typical nanodiamond. The clearly visible crystalline facets indicate a high quality of the nanodiamond. (c) Schematic illustration of the experimental setup. The 690-nm diode laser is used for PL measurement, the Ti:sapphire laser in the cw mode is used for PLE excitation and g^2 measurement. The pulsed Ti:sapphire laser is used for lifetime measurement. For a detailed description, please refer to the main text.

stage and the stacked XYZ steppers are placed in a cryostat, which is used to stabilize the sample temperature at 4 K. A homebuilt confocal microscope is used to focus the excitation laser beam onto the diamond surface through a microscope objective [numerical aperture (NA) 0.80, X100], which is also used to collect the fluorescence. A pair of polarizers is used for cross-polarization rejection of excitation laser light. A multimode fiber (50-μm core diameter, NA 0.22) is used to collect the signal. The collected signal is guided into a spectrometer with its 1800 grating/mm or towards two avalanche photodiodes for antibunching measurements.

To measure ensemble photoluminescence [Fig. 2(a)], a 690-nm laser is used for excitation and a 700-nm-long pass filter is placed on the collection arm to block residual 690-nm excitation light. For the photoluminescence-excitation (PLE) experiment, we use the Ti:sapphire laser with less than 5-MHz linewidth and a wide tunable wavelength range between 700–800 nm. The PLE scan experiment is performed through scanning a piezoetalon within a mode hop-free range of ~50 GHz and detects the off-resonant phonon sideband after a 750-nm-long pass filter. A wave meter is used to monitor the real-time wavelength of the exciting laser, as the feedback for the precisely locked laser wavelength at a specific value. With this method, the laser wavelength can be locked at the peak of the ZPL line of the single emitter, for the $g^2(\tau)$ and PLE stability measurements. Finally, lifetime measurements are recorded using a pulsed Ti:sapphire laser with a pulse length of ~10 ps.

III. RESULTS AND DISCUSSIONS

The measured spectrum of the SiV^- ensemble at 4 K is shown in Fig. 2(a). The ensemble represents different emitters that are present in the same nanocrystal. Since the confocal microscope has a finite resolution, we are not able to resolve individual emitters using the off-resonance excitation.

To probe individual emitters, we perform photoluminescence excitation (PLE). PLE measurement is an excellent enabler to probe individual emitters from an ensemble, since only the emitters resonating with an excitation source will be probed. Spectra of individual SiV defects are shown in Fig. 2(b). The spectra are obtained by sweeping the Ti:sapphire across a frequency range of the ensemble of SiVs as shown in Fig. 2(a). Figure 2(c) shows the fine structure of the SiV center. The four transitions are found to be correlated through measuring the spectrum of resonant fluorescence while tuning the excitation wavelength to be on resonant with the other four transitions.

To prove that only single emitters are probed, we choose a particular emitter at 738.949 84 nm [shown with a red arrow in Fig. 2(a)] and record the second-order autocorrelation measurement $g^2(\tau)$. The laser wavelength is scanned across the ZPL of this emitter and the measured $g^2(\tau)$ curve is shown in Fig. 2(d). The observed dip at zero delay time, $g^2(0) = 0.014 \pm 0.006$, satisfies the criteria of the single-photon emitter [$g^2(0) < 0.5$]. No background correction is performed and the data are fit to a two-level model [13]. Low $g^{(2)}(0)$ values are highly important to generating clean single-photon sources for quantum information [29]. The fluorescent lifetime of this defect is measured to be $T_1 = 1.126 \pm 0.005$ ns (141 MHz), as shown in Fig. 2(e), which is comparable to the lifetime ($0.92 + / - 0.06$ ns) derived from $g^2(\tau)$ fitting.

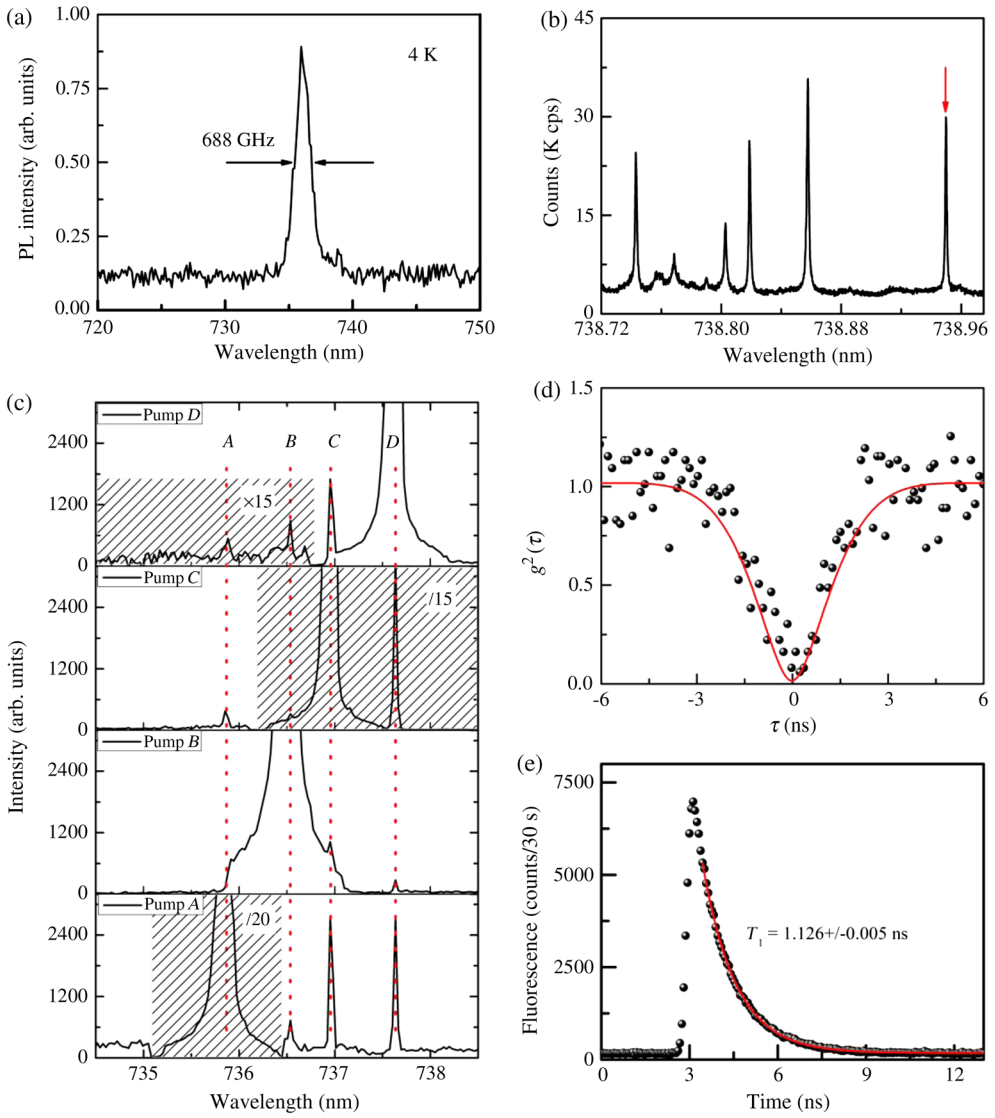

FIG. 2 (a) Off-resonant photoluminescence spectrum from a single nanodiamond recorded at 4 K using a 690-nm excitation laser. (b) Resonance fluorescence (PLE) spectrum of the sample showing several individual transitions of the SiV defects in a nanodiamond. Note that due to a close proximity of the SiVs in the nanodiamond, we are not able to absolutely specify which transitions are observed. (c) Fine structure of a single SiV center. If the excitation wavelength is tuned to be on resonant with one of the four individual transitions, the other three fluorescent peaks can be detected by the spectrometer. (d) Second-order correlation measurement $g^{(2)}(\tau)$ demonstrating that a single SiV defect is addressed. The $g^{(2)}(\tau)$ curve is recorded from the 738.949 83-nm line [red arrow in (b)]. The low excitation power (0.25 μW) is used to minimize the effect of power broadening. The phonon sideband is detected during $g^{(2)}(\tau)$ measurement. (e) Lifetime measurement of the same SiV center recorded using pulsed Ti: sapphire.

Figure 3(a) shows a high-resolution PLE spectrum of the same emitter using a low excitation power of 267 nW (~¼ of saturation power, as will be described later). The full width at half maximum (FWHM) of the PLE spectrum is only 325 ± 30 MHz, fit using a Lorentzian function. The observed value $\Gamma_{\mathrm{ND}} = 325 \pm 30$ MHz is relatively close to the lifetime-limited value of $1/2\pi T_1 = 141$ MHz and is comparable with values reported for SiV emitters occurring in bulk diamond [14,15,19]. It is also interesting to note that unlike the SiV, the typical linewidth for the nitrogen-vacancy centers in nanodiamonds is often significantly broader than the lifetime-limited value ($\Gamma_{\mathrm{ND}} \sim 1.2$ GHz in nanodiamonds vs $\Gamma_L \sim 16$ MHz lifetime limited) [25,26], making the SiV in nanodiamonds an attractive single-photon source.

To show the stability of the emitter, the same PLE scan is repeated 18 times. Figure 3(b) shows the ZPL line position at each scan. The standard frequency deviation from the ZPL resonance is only 24 MHz, which is smaller than one-tenth of the measured FWHM spectrum linewidth of the SiV^- center. Moreover, we do not observe the line position drifting away from the averaged line position, and the defect is stable for the duration of the measurements. We therefore conclude that spectral diffusion is negligible for these emitters, unlike the other color centers in nanodiamonds [26,27]. The absence of spectral diffusion can be attributed to the inversion symmetry of the SiV center [14,15]. The broadening of the PLE resonance is likely due to residual strain within the investigated nanodiamond or dipole-dipole interaction with the nearby SiV emitters in the same nanodiamond. We further study the emitters' stability under different

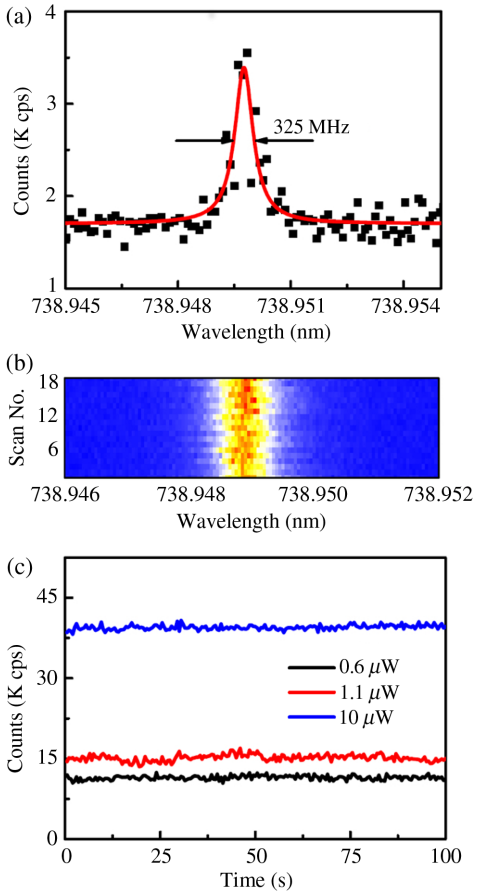

FIG. 3 (a) Photoluminescence excitation (PLE) of a single SiV at 4 K. The exciting laser wavelength is scanned through one of the resonant frequencies of one emitter while the PL from its phonon sideband (off resonant) is detected by an APD. In order to minimize the power broadening, an exciting power well below saturation power is used for this experiment. The 325-MHz FWHM linewidth is determined from Lorentz fitting to the PLE-scan-data curve. (b) An 18-times PLE scan is done to examine the spectrum stability of the emitter. Each scan takes ~2 min, and overall approximately 1 h to finish the 18 PLE scans. The ZPL line positions from the 18-times PLE measurement distribute around a mean value 738.949 83 nm with a standard deviation of 24 MHz. (c) The stability of the addressed SiV^- center is examined by locking the laser frequency to be on resonant with the defect, the monitored photon counts are stable at different excitation powers of 0.6 μW ($<P_s$),1.1 μW($\sim P_s$), and 10 μW($\gg P_s$). The sampling time of each point is 0.5 s.

excitation regimes—namely, below saturation, at saturation, and above saturation. The results are shown in Fig. 3(c). No blinking is observed, even for power exceeding 10 times the saturation power for the SiV. This emphasizes the remarkable photostability of the emitters, and the high quality of the host nanodiamond matrix. Combined with the nearly transform-limited lifetime, and negligible spectral diffusion, the SiV emitters in nanodiamonds can be ideal candidates for sensing, quantum-information science, and hybrid nanophotonics applications.

Figure 4 shows the counts and linewidth as a function of the excitation power. Resonant excitation is a very efficient method to drive the optical transition of individual emitters, hence power broadening of the ZPL linewidth is not negligible when exciting power is close to saturation or beyond it. The experiment is performed through repeated PLE scans across a ZPL wavelength for different exciting power ranging from 40 nW to 44 μW while detecting the phonon sideband with the avalanche photo diode (APD). From each of the scan data, the peak counts and FWHM linewidth data are obtained through Lorentzian fitting to the PLE scan data. The peak photon counting represents the value of the emitter when the laser is exactly on resonance. Figure 4(a) shows the plot of excitation laser power vs emitters' intensity. The peak count increases quickly when increasing the resonant exciting power within a small range from 40 nW to 10 μW, and reaches a steady state when exciting power is increased and beyond this range. The data are fitted well using equation

$$I(P) = I_\infty \frac{P/P_s}{1 + P/P_s}, \tag{1}$$

where $I(P)$ is the count rate, which depends on excitation power P. The two fitting parameters are saturation power P_s and the maximum count rate when the excitation power approaches infinite. The fitting results in a saturation power $P_s = 972 \pm 51$ nW for this single emitter, and a maximum count rate 35.3 ± 0.5 K cps.

Figure 4(b) shows the magnified region of the plot at lower excitation powers. FWHM data are fit well with a function of $\gamma_0 + \Gamma\sqrt{1 + P/P_s}$, where γ_0 is the constant value 24 MHz as we measure in spectral diffusion, P is the excitation laser power, and Γ is the linewidth when P vanishes. From the fitting, a minimum linewidth 312 ± 6 MHz is obtained for the low excitation power limit.

Finally, we investigate ZPLs of seventeen SiV centers in eight different nanodiamond crystals. The results are as shown in Table I. All investigated SiV centers have ZPL linewidths below 1 GHz, and none of them show blinking. The linewidths are measured through the PLE scan when the excitation power is set at P_s for each individual SiV center.

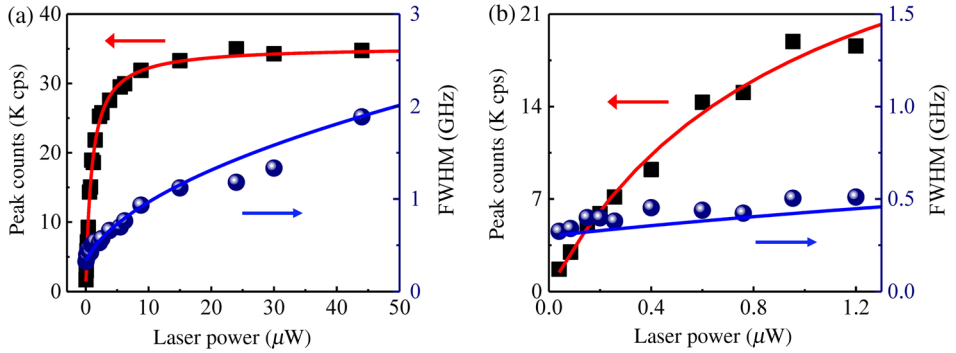

FIG 4 (a) Saturation curve of resonant photoluminescence of the single SiV^- center. The laser wavelength is scanned through the ZPL of the single emitter while detecting PL of the phonon sideband with an APD. The Lorentzian fit to all scan data is performed to extract the FHWH linewidth of ZPL and peak counts when the laser is on resonant with the single emitter. The resonant photoluminescence from an individual SiV^- saturates fast when the resonant excitation power is increased from 40 nW to 10 μW. The saturation power and saturation counts obtained from the fitting are 972 ± 51 nW and 35.3 ± 0.5 K cps separately. The ZPL linewidth (FWHM) of the single emitter approaches to a limit of 312 ± 6 MHz for zero exciting power, which is determined through the fitting function $\gamma_0 + \Gamma\sqrt{1 + P/P_s}$, to FWHM data. (b) Enlarged area of the lower excitation power regime.

TABLE I. Detailed study of 17 SiV centers. The lifetime and linewidth vary for different SiV emitters, however, no blinking is observed for all of them. The linewidths are measured through the PLE scan when the excitation power is set at P_s for each individual SiV center.

Crystal (number)	Emitter (number)	ZPL (nm)	Lifetime (ns)	Linewith (MHz)	Saturation counts (K cps)	Blinking
1	1	738.950	1.13	504	35.3	No
2	2	737.839	1.48	610	41.2	No
2	3	737.750	1.96	330	8.5	No
2	4	737.662	2.29	210	16.4	No
2	5	737.639	1.13	386	92	No
2	6	737.604	1.56	232	14.3	No
2	7	737.568	1.42	230	14	No
2	8	737.564	1.62	210	20	No
2	9	737.365	1.98	390	26.5	No
2	10	737.293	1.75	380	55.6	No
2	11	737.258	1.69	710	42	No
3	12	738.156	1.00	452	21.0	No
4	13	738.141	1.23	985	15.0	No
5	14	737.930	0.82	499	13.0	No
6	15	737.960	1.63	361	25.9	No
7	16	737.505	1.79	810	12.0	No
8	17	738.132	1.39	853	10.6	No

IV. SUMMARY

To summarize, we report on resonant excitation of single SiV defects in nanodiamonds. The emitters exhibit a nearly transform-limited linewidth of $\sim 325 \pm 30$ MHz at 4 K, only a factor of 2.3 broader that the lifetime-limited values of $\sim$141 MHz. Remarkably, minimal spectral diffusion and no blinking is observed, indicating the promising properties of the color centers in the grown CVD nanodiamonds. While further studies to investigate line broadening are important [30,31], our current results hold great promise to harness CVD-grown nanodiamonds hosting SiVs for coupling to photonic cavities and can be utilized for quantum-information processing. In addition, it will be interesting to investigate the SiV linewdith in molecular-sized nanodiamonds [32].

ACKNOWLEDGMENTS

We thank Kerem Bray and Russell Sandstrom for assistance with the CVD process. I. A. acknowledges support from the Australian Research Council Discovery Early Career Research Award (Project No. DE130100592). Partial funding for this research was provided by the

AOARD Grant No. FA2386-15-1-4044. W. B. G. acknowledges the strong support from the Singapore National Research Foundation through a Singapore 2015 NRF fellowship grant (No. NRF-NRFF2015-03) and its Competitive Research Programme (CRP Award No. NRF-CRP14-2014-02), and a start-up grant (No. M4081441) from Nanyang Technological University.

Note added.—Recently, we became aware that a similar work has appeared [33]. Our results are very comparable, both reporting nearly lifetime-limited linewidth from nanodiamonds. The main difference stems from the fact that we have not observed blinking in the emitter's fluorescence while the work by Jantzen *et al.* reports severe blinking of the Si*V*. This may originate from the different methods by which the nanodiamonds are synthesized (HPHT [33] vs CVD [our work]).

[1] R. Albrecht, A. Bommer, C. Deutsch, J. Reichel, and C. Becher, Coupling of a Single Nitrogen-Vacancy Center in Diamond to a Fiber-Based Microcavity, Phys. Rev. Lett. **110**, 243602 (2013).

[2] I. Aharonovich and E. Neu, Diamond nanophotonics, Adv. Opt. Mater. **2**, 911 (2014).

[3] A. W. Schell, H. Takashima, S. Kamioka, Y. Oe, M. Fujiwara, O. Benson, and S. Takeuchi, Highly efficient coupling of nanolight emitters to a ultra-wide tunable nanofibre cavity, Sci. Rep. **5**, 9619 (2015).

[4] D. D. Awschalom, L. C. Bassett, A. S. Dzurak, E. L. Hu, and J. R. Petta, Quantum spintronics: Engineering and manipulating atom-like spins in semiconductors, Science **339**, 1174 (2013).

[5] A. Ermakova, G. Pramanik, J. M. Cai, G. Algara-Siller, U. Kaiser, T. Weil, Y. K. Tzeng, H. C. Chang, L. P. McGuinness, M. B. Plenio, B. Naydenov, and F. Jelezko, Detection of a few metallo-protein molecules using color centers in nanodiamonds, Nano Lett. **13**, 3305 (2013).

[6] J. Wrachtrup, F. Jelezko, B. Grotz, and L. P. McGuinness, Nitrogen-vacancy centers close to surfaces, MRS Bull. **38**, 149 (2013).

[7] S. Kaufmann, D. A. Simpson, L. T. Hall, V. Perunicic, P. Senn, S. Steinert, L. P. McGuinness, B. C. Johnson, T. Ohshima, F. Caruso, J. Wrachtrup, R. E. Scholten, P. Mulvaney, and L. Hollenberg, Detection of atomic spin labels in a lipid bilayer using a single-spin nanodiamond probe, Proc. Natl. Acad. Sci. U.S.A. **110**, 10894 (2013).

[8] T. D. Merson, S. Castelletto, I. Aharonovich, A. Turbic, T. J. Kilpatrick, and A. M. Turnley, Nanodiamonds with silicon vacancy defects for nontoxic photostable fluorescent labeling of neural precursor cells, Opt. Lett. **38**, 4170 (2013).

[9] B. M. Chang, H. H. Lin, L. J. Su, W. D. Lin, R. J. Lin, Y. K. Tzeng, R. T. Lee, Y. C. Lee, A. L. Yu, and H. C. Chang, Highly fluorescent nanodiamonds protein-functionalized for cell labeling and targeting, Adv. Funct. Mater. **23**, 5737 (2013).

[10] E. H. Chen, O. Gaathon, M. E. Trusheim, and D. Englund, Wide-field multispectral super-resolution imaging using spin-dependent fluorescence in nanodiamonds, Nano Lett. **13**, 2073 (2013).

[11] C. Hepp, T. Müller, V. Waselowski, J. N. Becker, B. Pingault, H. Sternschulte, D. Steinmüller-Nethl, A. Gali, J. R. Maze, M. Atatüre, and C. Becher, Electronic Structure of the Silicon Vacancy Color Center in Diamond, Phys. Rev. Lett. **112**, 036405 (2014).

[12] E. Neu, R. Albrecht, M. Fischer, S. Gsell, M. Schreck, and C. Becher, Electronic transitions of single silicon vacancy centers in the near-infrared spectral region,Phys. Rev. B **85**, 245207 (2012).

[13] E. Neu, D. Steinmetz, J. Riedrich-Moeller, S. Gsell, M. Fischer, M. Schreck, and C. Becher, Single photon emission from silicon-vacancy centres in CVD-nano-diamonds on iridium, New J. Phys. **13**, 025012 (2011).

[14] L. J. Rogers, K. D. Jahnke, T. Teraji, L. Marseglia, C. Müller, B. Naydenov, H. Schauffert, C. Kranz, J. Isoya, L. P. McGuinness, and F. Jelezko, Multiple intrinsically identical single-photon emitters in the solid state, Nat. Commun. **5**, 4739 (2014).

[15] A. Sipahigil, K. D. Jahnke, L. J. Rogers, T. Teraji, J. Isoya, A. S. Zibrov, F. Jelezko, and M. D. Lukin, Indistinguishable Photons from Separated Silicon-Vacancy Centers in Diamond, Phys. Rev. Lett. **113**, 113602 (2014).

[16] T. Müller, C. Hepp, B. Pingault, E. Neu, S. Gsell, M. Schreck, H. Sternschulte, D. Steinmüller-Nethl, C. Becher, and M. Atatüre, Optical signatures of silicon-vacancy spins in diamond, Nat. Commun. **5**, 3328 (2014).

[17] J. C. Lee, I. Aharonovich, A. P. Magyar, F. Rol, and E. L. Hu, Coupling of silicon-vacancy centers to a single crystal diamond cavity, Opt. Express **20**, 8891 (2012).

[18] J. Riedrich-Möller, C. Arend, C. Pauly, F. Mücklich, M. Fischer, S. Gsell, M. Schreck, and C. Becher, Deterministic coupling of a single silicon-vacancy color center to a photonic crystal cavity in diamond, Nano Lett. **14**, 5281 (2014).

[19] R. E. Evans, A. Sipahigil, D. D. Sukachev, A. S. Zibrov, and M. D. Lukin, Coherent Optical Emitters in Diamond Nanostructures via Ion Implantation, Phys. Rev. Applied **5**, 044010 (2016).

[20] J. P. Goss, R. Jones, S. J. Breuer, P. R. Briddon, and S. Oberg, The Twelve-Line 1.682 eV Luminescence Center in Diamond and the Vacancy-Silicon Complex, Phys. Rev. Lett. **77**, 3041 (1996).

[21] O. Benson, Assembly of hybrid photonic architectures from nanophotonic constituents, Nature (London) **480**, 193 (2011).

[22] E. Perevedentseva, Y.-C. Lin, M. Jani, and C.-L. Cheng, Biomedical applications of nanodiamonds in imaging and therapy, Nanomedicine **8**, 2041 (2013).

[23] J. Wolters, A. Schell, G. Kewes, N. Nusse, M. Schoengen, H. Doscher, T. Hannappel, B. Lochel, M. Barth, and O. Benson, Enhancement of the zero phonon line emission from a single nitrogen vacancy center in a nanodiamond via

coupling to a photonic crystal cavity, Appl. Phys. Lett. **97**, 141108 (2010).

[24] L. Liebermeister, F. Petersen, A. v. Münchow, D. Burchardt, J. Hermelbracht, T. Tashima, A. W. Schell, O. Benson, T. Meinhardt, A. Krueger, A. Stiebeiner, A. Rauschenbeutel, H. Weinfurter, and M. Weber, Tapered fiber coupling of single photons emitted by a deterministically positioned single nitrogen vacancy center, Appl. Phys. Lett. **104**, 031101 (2014).

[25] Y. Shen, T. M. Sweeney, and H. Wang, Zero-phonon linewidth of single nitrogen vacancy centers in diamond nanocrystals, Phys. Rev. B **77**, 033201 (2008).

[26] H.-Q. Zhao, M. Fujiwara, M. Okano, and S. Takeuchi, Observation of 1.2-GHz linewidth of zero-phonon-line in photoluminescence spectra of nitrogen vacancy centers in nanodiamonds using a Fabry-Perot interferometer, Opt. Express **21**, 29679 (2013).

[27] P. Siyushev, V. Jacques, I. Aharonovich, F. Kaiser, T. Müller, L. Lombez, M. Atatüre, S. Castelletto, S. Prawer, F. Jelezko, and J. Wrachtrup, Low-temperature optical characterization of a near-infrared single-photon emitter in nanodiamonds, New J. Phys. **11**, 113029 (2009).

[28] A. Stacey, I. Aharonovich, S. Prawer, and J. E. Butler, Controlled synthesis of high quality micro/nano-diamonds by microwave plasma chemical vapor deposition, Diamond Relat. Mater. **18**, 51 (2009).

[29] X. Ding, Y. He, Z. C. Duan, N. Gregersen, M. C. Chen, S. Unsleber, S. Maier, C. Schneider, M. Kamp, S. Höfling, C.-Y. Lu, and J.-W. Pan, On-Demand Single Photons with High Extraction Efficiency and Near-Unity Indistinguishability from a Resonantly Driven Quantum Dot in a Micropillar, Phys. Rev. Lett. **116**, 020401 (2016).

[30] K. D. Jahnke, A. Sipahigil, J. M. Binder, M. W. Doherty, M. Metsch, L. J. Rogers, N. B. Manson, M. D. Lukin, and F. Jelezko, Electron–phonon processes of the silicon-vacancy centre in diamond, New J. Phys. **17**, 043011 (2015).

[31] C. Arend, J. N. Becker, H. Sternschulte, D. Steinmüller-Nethl, and C. Becher, Photoluminescence Excitation and Spectral Hole Burning Spectroscopy of Silicon Vacancy Centers in Diamond, Phys. Rev. Applied **5**, 044010 (2016).

[32] I. I. Vlasov, A. A. Shiryaev, T. Rendler, S. Steinert, S.-Y. Lee, D. Antonov, M. Voros, F. Jelezko, A. V. Fisenko, L. F. Semjonova, J. Biskupek, U. Kaiser, O. I. Lebedev, I. Sildos, P. R. Hemmer, V. I. Konov, A. Gali, and J. Wrachtrup, Molecular-sized fluorescent nanodiamonds, Nat. Nanotechnol. **9**, 54 (2014).

[33] U. Jantzen, A. B. Kurz, D. S. Rudnicki, C. Schäfermeier, K. D. Jahnke, U. L. Andersen, V. A. Davydov, V. N. Agafonov, A. Kubanek, L. J. Rogers, and F. Jelezko, Nanodiamonds carrying quantum emitters with almost lifetime-limited linewidths, New J. Phys. **18**, 073036 (2016).